Biodistribution and Radiation Dosimetry for ^{68}Ga-DOTA-CCK-66, a Novel CCK_2R-Targeting Compound for Imaging of Medullary Thyroid Cancer

Oliver Viering, MD, Andreas Rinscheid, PhD,† Nadine Holzleitner, PhD,‡ Alexander Dierks, MD,* Malte Kircher, MD,* Georgine Wienand,* Marianne Patt,* Hans-Jürgen Wester, PhD,‡ Ralph A. Bundschuh, MD, PhD,* Thomas Günther, PhD,‡|| Constantin Lapa, MD,*§ and Christian H. Pfob, MD**

Abstract: Cholecystokinin 2 receptor (CCK_2R) is a promising target for imaging and treatment of medullary thyroid cancer due to its overexpression in over 90% of tumor cells. ^{68}Ga-DOTA-CCK-66 is a recently introduced PET tracer selective for CCK_2R, which has shown favorable pharmacokinetics in vivo in preclinical experiments. In order to further investigate safety and suitability of this tracer in the human setting, whole-body distribution and radiation dosimetry were evaluated.

Patients and Methods: Six patients with a history of medullary thyroid cancer were injected intravenously with 169 ± 19 MBq of ^{68}Ga-DOTA-CCK-66. Whole-body PET/CT scans were acquired at 10 minutes, 1 hour, 2 hours, and 4 hours after tracer injection. Time-activity curves per organ were determined, and mean organ-absorbed doses and effective doses were calculated using OLINDA/EXM.

Results: Injection of a standard activity of 150 MBq of ^{68}Ga-DOTA-CCK-66 results in an effective dose of 4.5 ± 0.9 mSv. The highest absorbed organ doses were observed in the urinary bladder wall (40 mGy) and the stomach (15 mGy), followed by the kidneys (6 mGy), as well as the liver and the spleen (3 mGy each). CCK_2R-expressing tumor manifestations could be detected in 2 of the 6 patients, including lymph node, bone, and liver metastases.

Conclusions: ^{68}Ga-DOTA-CCK-66 exhibits a favorable dosimetry. Beyond physiologic receptor expression of the stomach, no other relevant tracer accumulation could be observed, rendering this organ at risk in case of subsequent radioligand therapy using ^{177}Lu-DOTA-CCK-66.

Key Words: medullary thyroid cancer, CCK_2R, theranostics, PET/CT imaging, dosimetry

Medullary thyroid cancer (MTC) is a rare neuroendocrine tumor arising from the parafollicular cells of the thyroid gland and accounts for approximately 1%–2% of all thyroid cancers. Since patients with MTC can only be cured by complete resection of the primary tumor and any locoregional or distant metastases, accurate disease staging is mandatory.[1] In advanced disease, both nonselective multikinase and selective RET inhibitors are approved and have shown significant effects on disease response and progression-free survival.[2,3] However, they may cause serious side effects and/or induce resistance,[4,5] so other treatment options remain desirable.

Regarding imaging, standard imaging procedures like whole-body CT, MRI, or bone scintigraphy often fail to detect MTC metastases.[1,6,7] The commonly used PET/CT tracers, ^{18}F-FDG and ^{18}F-DOPA, show sensitivities for detecting MTC lesions of around 59%–72%.[8] Even if the detection rate for ^{18}F-DOPA increases to more than 85% in patients with calcitonin levels above 150 pg/mL and calcitonin doubling times shorter than 24 months,[8,9] there is no therapeutic analog available for this compound for subsequent radioligand therapy (RLT).

Cholecystokinin 2 receptor (CCK_2R) is overexpressed in over 90% of MTC cases,[10] making it a promising target for diagnostic imaging and targeted therapy. Various compounds designed to target this specific receptor have been developed over the past years,[11–14] but there are just few data available for CCK_2R-targeting tracers suitable for PET/CT imaging.[15] We recently reported on the development and initial translation of the new minigastrin analog, ^{68}Ga-DOTA-CCK-66, which revealed promising preclinical characteristics, particularly in terms of high in vivo stability and rapid activity clearance from off-target tissue,[16] and thus, promising first preliminary clinical experience in 2 patients with advanced MTC.[16,17] Since this vector can also be labeled with therapeutic nuclides like lutetium-177 or actinium-225, DOTA-CCK-66 can also serve as a therapeutic option.

To assess the safety of ^{68}Ga-DOTA-CCK-66 as well as its diagnostic potential, biodistribution, and dosimetry, we here report the first PET/CT imaging data with this new probe in a small cohort of patients with MTC in a pilot study.

From the *Nuclear Medicine, Faculty of Medicine, University of Augsburg, Augsburg, Germany; †Medical Physics and Radiation Protection, University Hospital Augsburg, Augsburg, Germany; ‡TUM School of Natural Sciences, Department of Chemistry, Chair of Pharmaceutical Radiochemistry, Technical University of Munich, Garching, Germany; §Bavarian Cancer Research Center; and ||Molecular Imaging Program at Stanford, Department of Radiology, School of Medicine, Stanford University, Stanford, CA.

O.V., A.R., C.L., and C.H.P. contributed equally.

Conflicts of interest and sources of funding: A patent application on CCK_2R-targeted compounds including DOTA-CCK-66 with T.G., N.H., C.L., and H.J.W. as inventors has been filed. H.J.W. is founder and shareholder of Scintomics GmbH, Munich, Germany. No other potential conflicts of interest relevant to this article exist. This study has been funded by Deutsche Forschungsgemeinschaft (DFG, German Research Foundation—461577150).

Author contributions: All authors contributed to the study conception and design. Material preparation, data collection, and analysis were performed by O.V. and A.R. The first draft of the manuscript was written by O.V., A.R., and C.L., and all authors commented on previous versions of the manuscript. All authors read and approved the final manuscript.

Ethics approval: This study was performed in line with the principles of the Declaration of Helsinki. Approval was granted by the local Ethics Committee of Ludwig-Maximilians-Universität München (Munich, Germany; Date: 18.08.2023; No.: 23-0627).

Consent to participate: Informed consent was obtained from all individual participants included in the study.

Correspondence to: Constantin Lapa, MD, Nuclear Medicine, Faculty of Medicine, University of Augsburg, Stenglinstraße 2, 86156 Augsburg, Germany. E-mail: constantin.lapa@uk-augsburg.de.

Supplemental digital content is available for this article. Direct URL citation appears in the printed text and is provided in the HTML and PDF versions of this article on the journal's Web site (www.nuclearmed.com).

PATIENTS AND METHODS

Research Design and Subjects

Six patients (man 4 female; mean age ± SD, 54 ± 10 years) with a history of MTC underwent ^{68}Ga-DOTA-CCK-66 PET/CT for either restaging purposes or to evaluate a potential therapeutic option with CCK_2R-directed RLT. All patients showed elevated or rising tumor marker levels (mean calcitonin ± SD, 131 ± 120 pg/mL; mean calcitonin doubling time ± SD, 34 ± 26 months; mean CEA ± SD, 2.5 ± 1.6 ng/mL) at the time of PET/CT imaging. All patients exhibited a normal kidney function. Safety was assessed by monitoring adverse events up to 4 hours after injection of ^{68}Ga-DOTA-CCK-66. Detailed patient characteristics are presented in Supplemental Table 1, http://links.lww.com/CNM/A485. Two patients of the current cohort have already been presented in Günther et al.[16]

Preparation of the CCK_2-Targeting Probe ^{68}Ga-DOTA-CCK-66

The synthesis of ^{68}Ga-DOTA-CCK-66 was completed as previously described.[16]

PET Imaging

All ^{68}Ga-DOTA-CCK-66 scans were obtained on a dedicated PET/CT scanner (Biograph mCT 40; Siemens Healthineers, Erlangen, Germany or GE Discovery MI, GE HealthCare, Milwaukee, WI). Four whole-body scans (from the skull to the proximal thighs) were acquired at 10 minutes, 1 hour, 2 hours, and 4 hours after IV tracer injection (6 to 8 bed positions with an emission time of 2 minutes per bed position). All data were decay-corrected to the starting time of each individual scan. PET data sets were reconstructed using a standard reconstruction protocol provided by the manufacturer (2 iterations, 21 subsets), corrected for randoms, scatter, decay, and attenuation (using whole-body auxiliary CT, 35 mAs, 120 keV, a 512 × 512 matrix, 5-mm slice thickness, increment of 30 mm/s, rotation time of 0.5 seconds, and pitch of 0.8).

The PET scanners are periodically checked for calibration accuracy as part of quality control according to published guidelines and are accredited by European Association of Nuclear Medicine Research Ltd.[18]

Imaging and Dosimetry

Whole-organ volumes of interest (VOIs) were drawn for heart, kidneys, liver, spleen, stomach, lumbar vertebrae 2–4, and

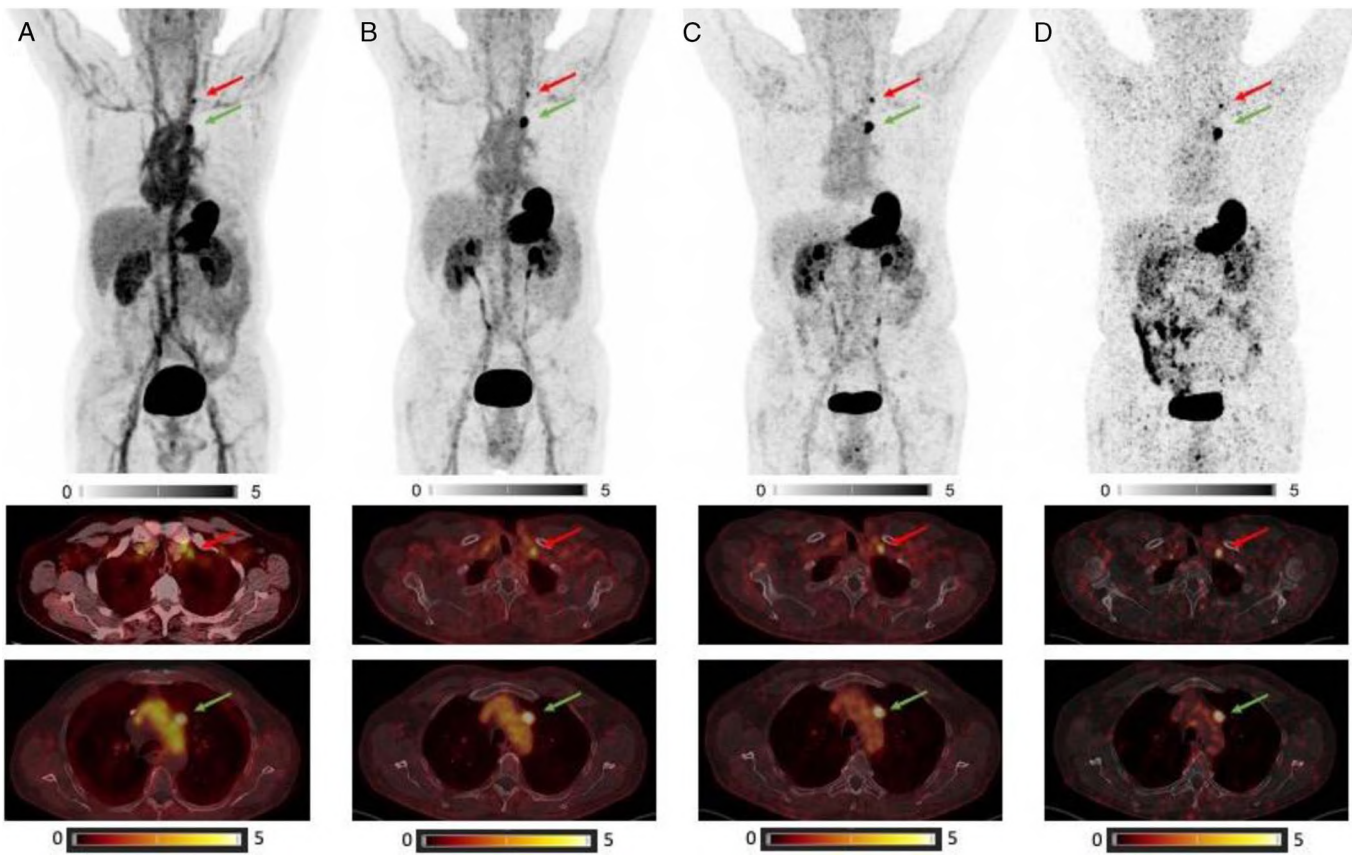

FIGURE 1. Sequential scans of a 64-year-old male patient who had initially undergone thyroidectomy and cervical lymph node dissection. After several local and lymphonodal recurrences, the patient presented with a rising calcitonin level of 110 pg/mL and a calcitonin doubling time of 16 months at the time of PET/CT imaging. MIPs (upper row) and fused transaxial PET/CT slices (lower rows) at (**A**) 10 minutes, (**B**) 1 hour, (**C**) 2 hours, and (**D**) 4 hours after tracer injection are displayed. Tracer uptake in CCK_2R-expressing lymph nodes could be observed already at 10 minutes and up to 4 hours after injection in the left retroclavicular region (10 minutes SUV_{max} 5.0; 4 hours SUV_{max} 8.0, red arrows) and in the upper mediastinum (10 minutes SUV_{max} 9.0; 4 hours SUV_{max} 23.5, green arrows).

the whole patient within the field of view on the first PET/CT scan using Simplicity^{90}Y (Mirada Medical and Boston Scientific). After coregistration, the VOIs were transferred to all quantified PET/CT images to determine the activity within each VOI for each time point. For the estimation of the activity of the red bone marrow, it was assumed that 6.7% of the red bone marrow is contained within lumbar vertebrae 2–4.[19] Monoexponential and monoexponential functions plus a constant were fitted to each time-activity data set using NUKFIT software.[20] A systematic uncertainty of the activity values of 10% was assumed. Optimal fit function was selected considering visual inspection and the uncertainties of the fit parameters (less than 50% of the value). Time-integrated activity coefficients (TIACs) were analytically calculated by integration of the time-activity curves. For the cases in which both fit functions could be used, the higher TIAC was used to obtain an upper estimate of the absorbed dose. The maximal deviation between the TIACs using the 2 fit functions was below 10%. For the stomach, decay-corrected activity within the VOIs was increasing for all time points. Thus, a trapezoidal integration from zero to the last time point with a following exponential decrease with the physical decay constant was used. The TIAC of the whole body was determined by using a scaling factor estimated from the administered activity and the decay-corrected activity within the field of view of the first PET/CT scan (before micturition). The TIAC of the urinary bladder was calculated by using the clearance rate of the remainder as filling rate and a bladder voiding interval. The following voiding interval was assumed: first voiding after 1 hour after injection and every 3.5 hours from then on, which reflects a realistic clinical setting. The TIACs for the urinary bladder were calculated by numerical integration from zero to 15 hours after injection using Excel (Microsoft Corporation).

Absorbed organ doses were calculated using OLINDA/EXM version 1.0.[21] Individual organ weights for heart, kidneys, liver, spleen, and total body weight were considered. For red bone marrow, a mass of 1500 g was assumed.[22]

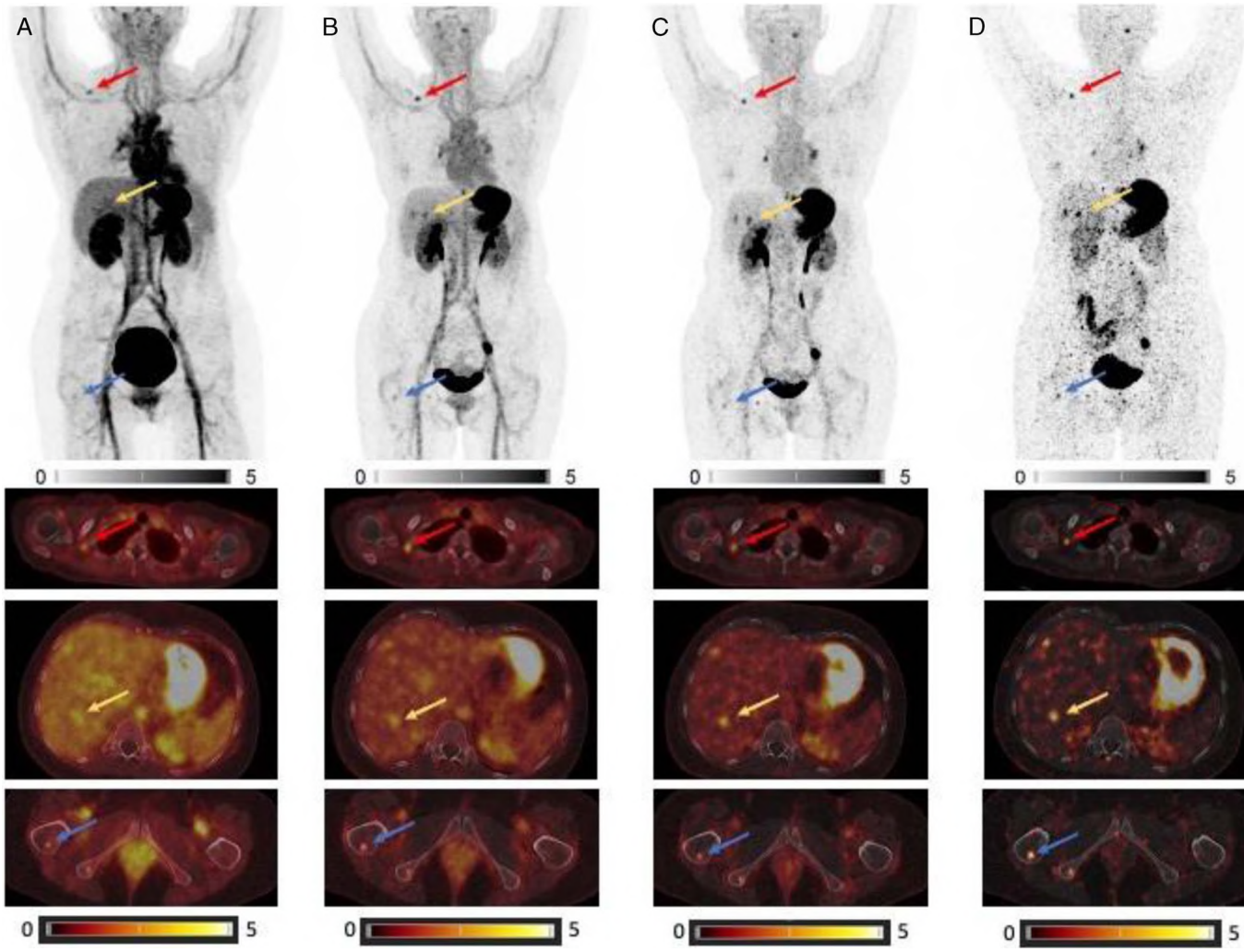

FIGURE 2. Sequential scans of a 46-year-old woman MTC patient who had undergone thyroidectomy and cervical lymph node dissection, as well as external beam radiation of the thyroid bed due to local tumor remnants. The patient showed a rising calcitonin level of 380 pg/mL and a calcitonin doubling time of 5 months at the time of PET/CT imaging. MIPs (upper row) and fused transaxial slices (lower rows) at (**A**) 10 minutes, (**B**)1 hour, (**C**) 2 hours, and (**D**) 4 hours after tracer injection are displayed. ^{68}Ga-DOTA-CCK-66 PET detected several lymph node metastases (eg, right retroclavicular, 10 minutes SUV_{max} 3.2; 4 hours SUV_{max} 4.9, red arrows), liver metastases (ie, in the right liver lobe segment VI, 10 minutes SUV_{max} 3.8; 4 hours SUV_{max} 6.7, yellow arrows), and bone metastases (ie, right femur, 10 minutes SUV_{max} 2.1; 4 hours SUV_{max} 4.3, blue arrows).

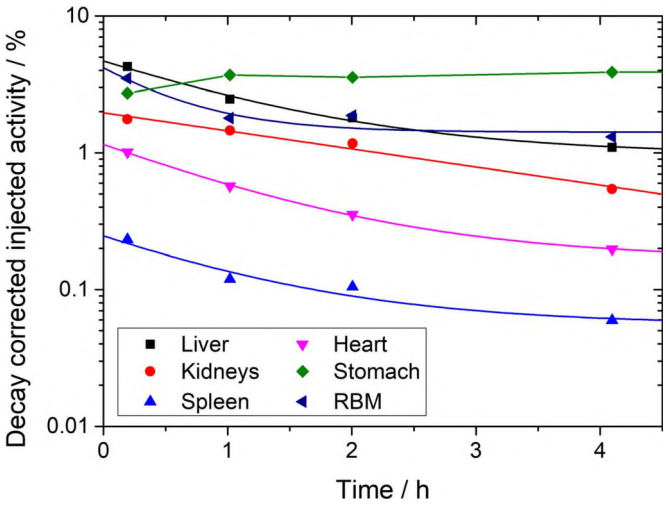

FIGURE 3. Time activity curves for patient 1 for major organs. An increasing decay-corrected tracer uptake over time was only observed in the stomach. In all other organs, decay-corrected activity uptake declined from early to late imaging.

For all other organs, the organ weights integrated in OLINDA/EXM were used. The effective dose was determined based on the current tissue weighting factors of ICRP 103.[23]

Semiquantitative analysis of visually detectable lesions was also done by VOIs. Corresponding SUV_{max} was recorded for the various time points. For estimation of background activity, a sphere with a diameter of 2 cm was placed within normal liver tissue. For assessment of the optimal imaging time point, tumor-to-background ratios (TBRs) were calculated for each time point by dividing SUV_{max} of tumor lesions by background SUV_{mean}.

Quantitative data are presented as the mean ± standard deviation (SD), as appropriate.

RESULTS

Radioligand and Patients

The administered amount of substance of ^{68}Ga-DOTA-CCK-66 was 18 µg. The overall injected activity was 169 ± 19 MBq with a specific activity greater than 9 MBq/µg. Injection of ^{68}Ga-DOTA-CCK-66 was well tolerated by all subjects, and no side effects or changes in vital signs were observed during the tracer's slow IV injection (~2 minutes), or thereafter (with a follow-up period of up to 4 hours).

Biodistribution

The biodistribution of ^{68}Ga-DOTA-CCK-66 was determined for all major organs in all patients. Figure 1 and Figure 2 show whole-body MIPs and transaxial sections of the 2 patients with detectable tumor lesions (P1, P6) at different time points. Figure 3 shows the time-activity curves for major organs expressed as percentage injected activity (%ID) for the same patient as in Figure 1 (P1). Comparable time-activity curves were recorded in all other patients.

An increasing tracer accumulation over time was only observed for the stomach, which can be attributed to physiological CCK_2R expression. The highest decay-corrected tracer uptake in the stomach and also in any other organ was observed in patient 3 with 20.8 %ID at 4 hours after injection. For all patients, the mean uptake of the stomach increased from 4.5 ± 4.3 %ID at 10 minutes to 7.6 ± 6.8 %ID at 4 hours. The mean uptake in the kidneys varied between 1.8 ± 0.4 %ID and 1.0 ± 0.3 %ID at 10 minutes and 4 hours after administration, respectively. Significant tracer uptake was also observed in the liver, with a mean uptake of 4.3 ± 0.6 %ID after 10 minutes, declining to 1.5 ± 0.5 %ID after 4 hours. Only low tracer uptake was observed for the red bone marrow with 2.6 ± 0.6 %ID at 10 minutes declining to 1.3 ± 0.4 %ID at 4 hours.

The decay-corrected urinary bladder content at 10 minutes after injection was about 9.6 ± 2.1%ID. All patients voided for the first time 40–60 minutes after administration of the radioligand.

Tumor Imaging and Tumor Marker Levels

Focal lesions consistent with malignancy were found in 2 patients (P1 and P6), whereas no suspicious tracer uptake could be detected in the other 4 individuals.

In brief, calcitonin levels were higher in the PET-positive patients with 110 pg/mL and 380 pg/mL, respectively, as compared with 73 ± 52 pg/mL in the PET-negative group. Also, a shorter calcitonin doubling time could be observed in the PET-positive patients with a calcitonin doubling time of 16 and 5 months as compared with 42 and 73 months in the PET-negative patients. CEA was only slightly elevated in 1 patient, who was CCK_2R negative.

In ^{68}Ga-DOTA-CCK-66 PET/CT, both PET-positive subjects presented with suspicious CCK_2R-expressing lymph nodes in the cervical and/or thoracic region. In patient 6, additional liver and bone metastases could be observed. A total of 12 lesions could be detected, including 5 CCK_2R-expressing lymph nodes, 3 liver lesions, and 4 bone lesions. Semiquantitative assessment of tumor SUV_{max} and TBR demonstrated an increase for lymph node, bone, and liver metastases over time, respectively. An overview of the SUV_{max} and TBR for the different tumor sites is given in Table 1, Table 2, and Supplemental Figure 1, http://links.lww.com/CNM/A485. Individual values for each CCK_2R-expressing lesion are presented in Supplemental Table 2, http://links.lww.com/CNM/A485.

TABLE 1. Tracer Uptake (SUV_{max}) in Visible Tumor Lesions and Background Uptake (SUV_{mean} in the Normal Liver Tissue) in Patient 1 and Patient 6 for Different Imaging Time Points.

	SUV_{max}			
	10 min Mean (Range)	**1 h Mean (Range)**	**2 h Mean (Range)**	**4 h Mean (Range)**
Lymph nodes (n = 5)	4.8 (3.2–9.0)	6.5 (3.3–14.1)	6.9 (4.0–13.2)	9.4 (3.5–23.5)
Hepatic lesions (n = 3)	3.8 (3.7–3.9)	3.6 (3.2–4.0)	3.9 (3.3–4.3)	5.4 (3.2–6.7)
Bone lesions (n = 4)	2.6 (1.6–4.3)	2.6 (1.9–3.8)	3.3 (2.4–5.2)	4.7 (4.2–6.2)
All lesions (n = 12)	3.8 (1.6–9.0)	4.5 (1.9–14.1)	4.9 (2.4–13.2)	6.8 (3.2–23.5)
SUV_{mean} background	2.2 (2.1–2.2)	1.5 (1.4–1.5)	1.1 (0.9–1.2)	0.5 (0.4–0.5)

TABLE 2. Comparison of TBR Determined by Dividing Average SUV_{max} of Tumor Lesions by Average SUV_{mean} of Background Tissue (as Measured in the Normal Liver Tissue) for Different Scanning Times

	TBR			
	10 min	1 h	2 h	4 h
Lymph nodes (n = 5)	2.2	4.5	6.5	20.9
Hepatic lesions (n = 3)	1.8	2.5	3.7	11.9
Bone lesions (n = 4)	1.2	1.8	3.1	10.5
All lesions (n = 12)	1.8	3.1	4.7	15.2

Dosimetry

Time-integrated activity coefficients of segmented organs were calculated for each patient individually. In addition, the mean values for all patients are given in Table 3. The highest number of disintegrations per organ occurred in the stomach and urinary bladder, with an average TIAC of 0.10 ± 0.09 hours (stomach) and 0.18 ± 0.06 hours (urinary bladder). The average absorbed dose/dose coefficients across all subjects are shown in Table 4. The highest absorbed dose per unit activity was observed in the urinary bladder wall (0.269 ± 0.103 mGy/MBq), followed by the stomach (0.098 ± 0.077 mGy/MBq), the kidneys (0.039 ± 0.019 mGy/MBq), as well as the liver and the spleen (both 0.018 ± 0.003 mGy/MBq).

The effective dose was individually determined for each patient using the current tissue-weighting factors from ICRP 103.[23]

On average, the effective dose coefficient was 0.030 ± 0.006 mSv/MBq. Thus, the effective dose for a standard injection of 150 MBq of ^{68}Ga-DOTA-CCK-66 results in about 4.5 ± 0.9 mSv. For comparison, the effective dose coefficient using the outdated tissue-weighting factors from ICRP 60[24] as provided by OLINDA/EXM was 0.033 ± 0.006 mSv/MBq.

Table 5 provides an overview of absorbed doses for selected organs and effective doses for a typically injected activity for ^{68}Ga-DOTA-CCK-66 and other commonly used PET tracers.

Discussion

Given the clinical need for improved imaging and therapy modalities for staging and treatment of MTC patients, we recently reported on a new CCK_2R-targeting compound.[16] Preclinical results suggested high in vivo stability and rapid activity clearance from off-target tissue,[16] which could be also observed in preliminary proof-of-concept studies previously reported.[16,17] In order to further examine the clinical value of ^{68}Ga-DOTA-CCK-66, we here investigated its biodistribution and dosimetry in 6 MTC patients.

TABLE 3. TIACs for Major Organs for Each Patient Individually and Mean TIACs for All Patients

	TIACs (h)							
Source Organs	P1	P2	P3	P4	P5	P6	MW	SD
Liver	0.042	0.047	0.042	0.045	0.061	0.039	0.046	0.008
Kidneys	0.021	0.020	0.022	0.021	0.028	0.026	0.023	0.003
Spleen	0.002	0.008	0.005	0.006	0.006	0.006	0.006	0.002
Heart	0.009	0.009	0.010	0.008	0.012	0.010	0.010	0.001
Stomach	0.054	0.075	0.269	0.095	0.039	0.040	0.095	0.088
Urinary bladder	0.209	0.176	0.081	0.187	0.178	0.267	0.183	0.060
Red bone marrow	0.035	0.035	0.023	0.028	0.028	0.026	0.029	0.005
Remainder	0.710	0.808	0.981	0.760	0.822	0.490	0.762	0.161

TABLE 4. Absorbed Organ Dose Coefficients and Absorbed Organ Doses (for a Typical Amount of 150 MBq of ^{68}Ga-DOTA-CCK-66)

Target Organ	β (mGy/MBq)	Photon (mGy/MBq)	Total (mGy/MBq)	Absorbed Dose (mGy/150 MBq)
Adrenals	0.004	0.005	0.009	1.3 ± 0.3
Brain	0.004	0.002	0.006	0.9 ± 0.2
Breasts	0.004	0.002	0.006	0.9 ± 0.2
Gallbladder wall	0.004	0.005	0.009	1.4 ± 0.2
LLI wall	0.004	0.008	0.012	1.8 ± 0.3
Small intestine	0.004	0.006	0.010	1.5 ± 0.2
Stomach	0.085	0.013	0.098	15 ± 12
ULI wall	0.004	0.006	0.010	1.4 ± 0.2
Heart wall	0.009	0.004	0.013	2.0 ± 0.3
Kidneys	0.033	0.007	0.039	5.9 ± 2.9
Liver	0.013	0.005	0.018	2.6 ± 0.5
Lungs	0.004	0.003	0.007	1.1 ± 0.2
Muscle	0.004	0.004	0.008	1.2 ± 0.2
Ovaries	0.004	0.008	0.013	1.9 ± 0.2
Pancreas	0.004	0.007	0.011	1.7 ± 0.4
Red marrow	0.006	0.004	0.010	1.4 ± 0.2
Osteogenic cells	0.011	0.004	0.014	2.1 ± 0.4
Skin	0.004	0.002	0.006	0.9 ± 0.2
Spleen	0.012	0.006	0.018	2.7 ± 0.5
Testes	0.004	0.004	0.008	1.2 ± 0.2
Thymus	0.004	0.003	0.007	1.1 ± 0.2
Thyroid	0.004	0.003	0.007	1.0 ± 0.2
Urinary bladder wall*	0.232	0.038	0.269	40 ± 15
Uterus	0.004	0.013	0.018	2.7 ± 0.2
Total body	0.005	0.003	0.008	1.2 ± 0.3
Effective dose coefficient (mSv/MBq)			0.030	
Effective dose (mSv)				4.5 ± 0.9

*Voiding at 1 hour and 3.5 hours.

LLI, lower large intestine; ULI, upper large intestine.

As expected and in line with other previous used CCK_2R-targeting tracers,[12,14,15] ^{68}Ga-DOTA-CCK-66 was well tolerated by all patients. No acute or subacute adverse events were observed, and no significant changes in vital signs were noted. In line with preclinical data, a favorable biodistribution profile for ^{68}Ga-DOTA-CCK-66 was observed in all MTC patients, showing relevant uptake only in the CCK_2R-expressing stomach, whereas off-target accumulation was low or renally excreted within the first 4 hours. In 2 subjects with detectable MTC lesions, the highest lesion-to-background ratio was observed at 4 hours after administration of the radiopharmaceutical; however, for practical reasons and the fast decay of gallium-68, we recommend scanning the patients at 2 hours after administration of the compound, particularly because the lesion-to-background ratio is already well-suited for tumor detection.

In 2 of the 6 patients, pathologic tracer uptake consistent with MTC tumor manifestations was recorded. Although this finding might suggest a relatively low detection rate of ^{68}Ga-DOTA-CCK-66, it must be noted that the imaging was performed in a small and heterogeneous patient cohort. Therefore, the performance of ^{68}Ga-DOTA-CCK-66 needs to be verified in a larger group of

TABLE 5. Comparison of Absorbed Dose Coefficients and Effective Doses for ^{68}Ga-DOTA-CCK-66 and Commonly Used PET Tracers

		^{68}Ga-PSMA-I&T	^{18}F-FDG	^{68}Ga-DOTATOC	^{18}F-DOPA	^{68}Ga-DOTA-CCK-66
Targeted Organs	**Unit**	**Herrmann et al[25]**	**ICRP 106[26]**	**Sandström et al[27]**	**ICRP 106[26]**	**This work**
Kidneys	mSV/MBq	0.220	0.017	0.082	0.031	0.039
Stomach	mSV/MBq	0.011	0.011	-	0.010	0.098
Urinary bladder wall	mSV/MBq	0.067	0.130	0.119	0.300	0.269
Liver	mSV/MBq	0.043	0.021	0.041	0.009	0.018
Spleen	mSV/MBq	0.063	0.011	0.108	0.010	0.018
Effective dose coefficient	mSV/MBq	0.020	0.019	0.021	0.025	0.030
Typical injected activity	MBq	150	370	150	300	150
Effective dose	mSV	3.0	7.0	3.2	7.5	4.5

patients, especially in comparison to the current gold standard ^{18}F-DOPA. Since the CCK_2R PET-positive subjects exhibited higher calcitonin levels and shorter calcitonin doubling times than the CCK_2R PET-negative individuals, PET positivity and CCK_2R expression, respectively, could be linked to a more aggressive tumor biology, potentially rendering ^{68}Ga-DOTA-CCK-66 a noninvasive readout for tumor biology. Although no firm conclusions on this assumption can be drawn at this moment, further research especially in a larger number of patients is definitely warranted.

Since other PET tracers, such as ^{18}F-DOPA, can achieve good detection rates in progressive disease as well, the potential strength of DOTA-CCK-66 is the possibility of receptor-directed RLT using its ^{177}Lu- or even ^{225}Ac-labeled analog, a concept that has already been proven to be highly successful in the context of PSMA- or SSTR-directed RLT.[28,29] ^{68}Ga-DOTA-CCK-66 demonstrated a favorable biodistribution and dosimetry and could be a meaningful addition to the theranostic approach for patients with advanced MTC. Although kidneys and bone marrow are not considered to be organs at risk in CCK_2R-directed therapeutic approaches, the highest absorbed organ dose and the only one that increased over time was observed in the stomach due to its high physiological CCK_2R expression.[30] Dosimetry data for the latest promising CCK_2R-targeting compounds like DOTA-MGS5 or PP-F11N are scarce, rendering a comparison with DOTA-CCK-66 difficult. However, high and increasing SUV_{max} values over time for the stomach (1 hour: 21.5, 2 hours: 23.6) have also been observed for ^{68}Ga-DOTA-MGS5 in a recent work,[15] which corroborates our results. Dosimetry data for PP-F11N, which have already been investigated in a phase 0 and phase I study as a therapeutic agent, are only available for the ^{177}Lu-labeled agent. In a limited number of patients, it could be demonstrated that the maximum tolerable stomach dose (50 Gy) would not be exceeded with a cumulative activity of 50 GBq of ^{177}Lu-PP-F11N.[14,31,32] Although we assume this threshold would also not be exceeded in the context of therapeutic application using DOTA-CCK-66 as well, dosimetry and subsequent therapy data for ^{177}Lu-labeled DOTA-CCK-66 are needed.

CONCLUSIONS

Application of ^{68}Ga-DOTA-CCK-66 was well tolerated and showed a favorable biodistribution and dosimetry with high accumulation observed only in tumor lesions and the CCK_2R-expressing stomach, thus offering promising imaging characteristics. Given the inherent theranostic option of this approach, its high in vivo stability, and favorable overall preclinical data, further studies with this novel vector and its ^{177}Lu/^{225}Ac-labeled analog are highly warranted.

REFERENCES

1. Wells SA Jr., Asa SL, Dralle H, et al. American Thyroid Association guidelines task force on medullary thyroid carcinoma. Revised American Thyroid Association guidelines for the management of medullary thyroid carcinoma. *Thyroid*. 2015;25:567–610.
2. Wells SA Jr., Robinson BG, Gagel RF, et al. Vandetanib in patients with locally advanced or metastatic medullary thyroid cancer: a randomized, double-blind phase III trial. *J Clin Oncol*. 2012;30:134–141.
3. Hadoux J, Elisei R, Brose MS, et al. Phase 3 trial of selpercatinib in advanced RET-mutant medullary thyroid cancer. *N Engl J Med*. 2023;389:1851–1861.
4. Hadoux J, Schlumberger M. Chemotherapy and tyrosine-kinase inhibitors for medullary thyroid cancer. *Best Pract Res Clin Endocrinol Metab*. 2017;31:335–347.
5. Vodopivec DM, Hu MI. RET kinase inhibitors for RET-altered thyroid cancers. *Ther Adv Med Oncol*. 2022;14:17588359221101691.
6. Terroir M, Caramella C, Borget I, et al. F-18-Dopa positron emission tomography/computed tomography is more sensitive than whole-body magnetic resonance imaging for the localization of persistent/recurrent disease of medullary thyroid cancer patients. *Thyroid*. 2019;29:1457–1464.
7. Giraudet AL, Vanel D, Leboulleux S, et al. Imaging medullary thyroid carcinoma with persistent elevated calcitonin levels. *J Clin Endocrinol Metab*. 2007;92:4185–4190.
8. Giovanella L, Treglia G, Iakovou I, et al. EANM practice guideline for PET/CT imaging in medullary thyroid carcinoma. *Eur J Nucl Med Mol Imaging*. 2020;47:61–77.
9. Romero-Lluch AR, Cuenca-Cuenca JI, Guerrero-Vázquez R, et al. Diagnostic utility of PET/CT with ^{18}F-DOPA and ^{18}F-FDG in persistent or recurrent medullary thyroid carcinoma: the importance of calcitonin and carcinoembryonic antigen cutoff. *Eur J Nucl Med Mol Imaging*. 2017;44:2004–2013.
10. Reubi JC, Schaer JC, Waser B. Cholecystokinin(CCK)-a and CCK-B/gastrin receptors in human tumors. *Cancer Res*. 1997;57:1377–1386.
11. Behr TM, Béhé MP. Cholecystokinin-B/gastrin receptor-targeting peptides for staging and therapy of medullary thyroid cancer and other cholecystokinin-B receptor-expressing malignancies. *Semin Nucl Med*. 2002;32:97–109.
12. Lezaic L, Erba PA, Decristoforo C, et al. [^{111}In]in-CP04 as a novel cholecystokinin-2 receptor ligand with theranostic potential in patients with progressive or metastatic medullary thyroid cancer: final results of a GRAN-T-MTC phase I clinical trial. *Eur J Nucl Med Mol Imaging*. 2023;50:892–907.
13. Grossrubatscher E, Fanciulli G, Pes L, et al. Advances in the management of medullary thyroid carcinoma: focus on peptide receptor radionuclide therapy. *J Clin Med*. 2020;9:3507.
14. Rottenburger C, Nicolas GP, McDougall L, et al. Cholecystokinin 2 receptor agonist ^{177}Lu-PP-F11N for radionuclide therapy of medullary thyroid carcinoma: results of the Lumed phase 0a study. *J Nucl Med*. 2020;61:520–526.
15. von Guggenberg E, Uprimny C, Klinger M, et al. Preliminary clinical experience with cholecystokinin-2 receptor PET/CT using the ^{68}Ga-labeled minigastrin analog DOTA-MGS5 in patients with medullary thyroid cancer. *J Nucl Med*. 2023;64:859–862.
16. Günther T, Holzleitner N, Viering O, et al. Preclinical evaluation of minigastrin analogs and proof-of-concept [^{68}Ga]Ga-DOTA-CCK-66 PET/CT in 2 patients with medullary thyroid cancer. *J Nucl Med*. 2024;65:33–39.
17. Viering O, Günther T, Holzleitner N, et al. CCK2 receptor-targeted PET/CT in medullary thyroid cancer using [^{68}Ga]Ga-DOTA-CCK-66. *J Nucl Med*. 2024;65:493–494.

18. Huizing DMV, Koopman D, van Dalen JA, et al. Multicentre quantitative ^{68}Ga PET/CT performance harmonisation. *EJNMMI Phys*. 2019;6:19.
19. Herrmann K, Lapa C, Wester HJ, et al. Biodistribution and radiation dosimetry for the chemokine receptor CXCR4-targeting probe ^{68}Ga-pentixafor. *J Nucl Med*. 2015;56:410–416.
20. Kletting P, Schimmel S, Kestler HA, et al. Molecular radiotherapy: the NUKFIT software for calculating the time-integrated activity coefficient. *Med Phys*. 2013;40:102504.
21. Stabin MG, Sparks RB, Crowe E. OLINDA/EXM: the second-generation personal computer software for internal dose assessment in nuclear medicine. *J Nucl Med*. 2005;46:1023–1027.
22. Ferrer L, Kraeber-Bodéré F, Bodet-Milin C, et al. Three methods assessing red marrow dosimetry in lymphoma patients treated with radioimmunotherapy. *Cancer*. 2010;116(4 Suppl):1093–1100.
23. The 2007 Recommendations of the International Commission on Radiological Protection. ICRP publication 103. *Ann ICRP*. 2007;37(2–4):1–332.
24. 1990 Recommendations of the International Commission on Radiological Protection. *Ann ICRP*. 1991;21(1–3):1–201.
25. Herrmann K, Bluemel C, Weineisen M, et al. Biodistribution and radiation dosimetry for a probe targeting prostate-specific membrane antigen for imaging and therapy. *J Nucl Med*. 2015;56:855–861.
26. ICRP. Radiation dose to patients from radiopharmaceuticals. Addendum 3 to ICRP Publication 53. ICRP Publication 106. Approved by the Commission in October 2007. *Ann ICRP*. 2008;38(1–2):1–197.
27. Sandström M, Velikyan I, Garske-Román U, et al. Comparative biodistribution and radiation dosimetry of ^{68}Ga-DOTATOC and ^{68}Ga-DOTATATE in patients with neuroendocrine tumors. *J Nucl Med*. 2013;54:1755–1759.
28. Sartor O, de Bono J, Chi KN, et al. VISION investigators. Lutetium-177-PSMA-617 for metastatic castration-resistant prostate cancer. *N Engl J Med*. 2021;385:1091–1103.
29. Pavel M, Öberg K, Falconi M, et al. ESMO guidelines committee. Gastroenteropancreatic neuroendocrine neoplasms: ESMO clinical practice guidelines for diagnosis, treatment and follow-up. *Ann Oncol*. 2020;31:844–860.
30. Barrett TD, Lagaud G, Wagaman P, et al. The cholecystokinin CCK2 receptor antagonist, JNJ-26070109, inhibits gastric acid secretion and prevents omeprazole-induced acid rebound in the rat. *Br J Pharmacol*. 2012;166:1684–1693.
31. Emami B, Lyman J, Brown A, et al. Tolerance of normal tissue to therapeutic irradiation. *Int J Radiat Oncol Biol Phys*. 1991;21:109–122.
32. Rottenburger C, Nicolas G, McDougall L, et al. The CCK-2 receptor agonist Lu-177-PP-F11N for PRRT of medullary thyroid cancer—recent results of the phase 1 "LUMED" study. *Nuklearmedizin*. 2021;60:L15.